Effect of Gluon Damping Rate to the Viscosity Coefficient of the Quark-gluon Plasma at Finite Chemical potential

Hou Defu * Li Jiarong

September 16, 2018

Institute of Particle Physics, Hua-Zhong Normal University
Wuhan 430070, China
E-mail: hzipp@ccnu.edu.cn
* present address: Institute für theoretische physik,
93040 Uni Regensburg, Germany.
E-mail: defu.hou@rphs1.physik.uni-regensburg.de

Abstract

By considering the Debye screening and the damping rate of gluons, the viscosity cofficient of the quark-gluon plasma was evaluated via the real time finite temperature QCD in the relaxiation time approximation at finite temperature and chemical potential. The results show that both the damping rate and quark chemical potential cause considerable enhancements to the viscosity coefficient of the hot dense quark-gluon plasma.

PCAC number(s): 12.38.Mh, 12.38.Bx

1 Introduction

The calculation of the viscosity coeffcient in a hot and dense system is of interest both in the fields of high energy heavy ion collisions and astrophysics [1-4]. The dissipative processes in a quark-gluon plasma(QGP) supposed to be formed in ultrarelativetic heavy collision can be described by the viscosity coefficient.

Because of the estimated very short collision time of the ions in the heavy ion collisions, the equilibrium statistical approaches are probably inappropriate for an adequate description of such a process, and the dissipative phenomena are important, at least for the equilibration and the expansion phases of the system. In principle, the dissipative processes in heavy ion collisions should be described by non-equilibrium dynamical theory that is based on QCD.

There are two methods to calculate the shear viscosity in QGP. The first one is by use of the relativistic kinetic theory. Starting from the Boltzmann equation, the viscosity coefficient η can be derived containing the transport cross section[2,3]. The second one is from the kubo formulas[2]. For example, in the relaxation time approximation, the shear viscosity coefficient was found to be $\eta = cT^3/\alpha_s^2 \ln(1/\alpha_s)$, the constant c was estimated to be 1.02,0.28,or o.57,whereas a variational calculation gave c = 1.16 with two quark flavors in high temperature limit[2,3]. And Ref.3 also gave the result beyond the leading logarithm approximation,

$$\eta = \frac{T^3}{\alpha_s^2} \left[\frac{0.11}{\ln(\frac{0.19}{\alpha_s})} + \frac{0.37}{\ln(\frac{0.21}{\alpha_s})} \right].$$

On the other hand , basing on the kubo formula, Ref.2 gave $\eta \leq 2.6 T^3/\alpha_s$ and the lattice calculations obtained the value near the phase transition as $0 \leq \eta/T^3 \leq 9.5$ [2].

It is known that the ensential nature of particles in a plasma at finite temperature is that they no longer have a infinite lifetimes, but have finite widths becaue of the collective effects. That is quite different from the behavior at zero temperature [6,7]. In QGP Debye screening and damping of collective modes occur because of the interactions among particles and the heat bath. Therefore it is reasonable to take into account both the Debye screening and finite width effects when study the collective behaviors of the QGP, which might also influence the transport processes of QGP.

On the other hand, so far most all of the results of the shear viscosity cofficients in QGP are calculated at finite temperature without taking into account of the baryon density. Certainly by lattice simulation it is difficult to include the baryon density ,which is related to the baryo-chemical potential μ_b through $\mu = \mu_b/3$ and measures the deviation from the balance of quarks and and antiquarks. However at RHIC energies,there might still exist a considerable amount of stopping to $\mu/T \sim 1 - 2[5]$, μ is the quark chemical potential.

In this paper we will investigate the damping rate effect of the transverse gluon on the shear viscosity coefficient of QGP at both finite temperature and chemical potential quark chemical potential. We will show explicitly both the finite width and chemical potential cause considerable enhancements to the shear viscosity.

The paper will be organized as follows. In Sec. II we will get the shear viscosity of quarks and gluons via real time QCD by considering both the Debye screening and finite width effects at finite chemical potential. In Sec.III we will consider the running behavior of the coupling constant ane present numerical results. Finally we will summarize our results in Sec.IV.

2 Calculation of the viscosity coefficent

We will calculate the shear viscosity coefficient by using the relativistic kinetic theory for a massless QGP in the so-called relaxation time approxima-

tion[2,3]:

$$\eta_i = \frac{4}{15} \varepsilon_i \lambda_i,\tag{1}$$

where ε_i is the energy density of particles of type i in the QGP and λ_i is the mean free path, which is the inverse interaction rate: $\lambda_i = \frac{1}{\Gamma_i}$. Considering the large angle scattering dominate the transport processes, we should multiply the interaction rate by a factor $\sin^2 \theta$,

$$\Gamma_{trsp.} = \int \sin^2 \theta \Gamma_i, \tag{2}$$

which is the so-called transport interaction rate, and θ is the scattering angle in the center of mass system.

There are two equivalent ways of computing the interaction rates either using the matrix elements or from imaginary parts of the quark or gluon self-energies [3].

$$\Gamma_i = -\frac{1}{4|p|} Im Tr(\not p \Sigma)|_{p_0 = E}. \tag{3}$$

Let us consider first the quark self-energy shown in fig.1, where we have included the screening effects and the damping rate effects by using the effective gluon propagator[8]. For hard quark momentum ($< p_q > \sim T$) it is sufficient to use the bare quark propagator and bare vertices. We will calculate the imaginary part of the self-energy at finite temperature and chemical potential using the Thermo Field Dynamics. For the hard particles one can show that the main contributions to the interaction rate comes from the soft momentum transfer range,i.e. $q \sim gT$ in the weak coupling limit[3].

Using the usual Feynman rules of QCD to evaluate the diagram of Fig.1, one can obtain:

$$Tr(\not p\Sigma) = -g^2 C_f \int \frac{d^D q}{(2\pi)^D} \frac{Tr(\not p\gamma^\mu(\not p + \not q)\gamma^\nu)}{(p+q)^2} \Delta_{\mu\nu}, \quad D = 4 - \epsilon, \quad (4)$$

where $\Delta_{\mu\nu}$ is the effective gluon propagator, in covariant gauge[9],

$$\Delta_{\mu\nu}(q) = A_{\mu\nu}(q)\Delta_T(q) + B_{\mu\nu}\Delta_L(q) + D_{\mu\nu}\Delta_{\xi}(q), \tag{5}$$

where

$$A_{\mu\nu}(q) = \delta_{\mu i} (\delta_{ij} - \frac{q_i q_j}{Q^2}) \delta_{j\nu}, \quad B_{\mu\nu} = (\delta_{\mu 0} - \frac{q_\mu q_0}{q^2}) \frac{q^2}{Q^2} (\delta_{\nu 0} - \frac{q_\nu q_0}{q^2})$$

$$D_{\mu\nu} = \frac{q_\mu q_\nu}{q^2}, \quad \Delta_{\xi} = \xi \frac{1}{q^2}, \quad \Delta_{T,L} = \frac{1}{q^2 - \Pi_{T,L}}, \tag{6}$$

where ξ is the gauge parameter.

In the static limit the contribution of the hard thermal loops for hot dense QCD are [5],

$$\Pi_L(q_0 \to 0, Q) = \Pi_{00}(q_0 \to 0, Q) = m_0^2 = g^2 T^2 \left(1 + \frac{N_f}{6} + \frac{1}{2\pi^2} \sum_f \frac{\mu_f^2}{T^2}\right) \quad (7)$$

for the longitudinal part and

$$\Pi_T(q_0 \to 0, Q) = 0 \tag{8}$$

for the transverse part of gluon polarization tensor. Substituting eqs.(7),(8) into eq(6),one gets

$$\Delta_L = \frac{1}{q^2 - m_0^2}, \quad \Delta_T = \frac{1}{q^2}.$$
(9)

In a thermal system, because of the thermal effects and the particles interactions, the particles (quasi-particles) will no longer have infinite lifetime, namely there are damping for the particles in QGP, which is an important feature of QGP. If one take into account the damping rate of the transverse gluon $\nu_T \sim N\alpha_s T[3,8]$, the transverse gluon propagator can be written as [6,7]

$$\Delta_T' = \frac{1}{(q_0 - i\nu_T)^2 - Q^2}. (10)$$

By using eqs(5)-(10),one can cast eq(4) into:

$$Tr(\not p\Sigma) = -g^2 C_f \int \frac{d^D q}{(2\pi)^D} \frac{2|P|^2}{(p+q)^2} (\Delta_T'(q) - \Delta_L(q) - (1-\xi) \frac{(\hat{P} \cdot \hat{Q})^2}{q^2}).$$
(11)

where
$$C_f = \frac{N^2 - 1}{2N}$$
.

For finite temperature QCD, we will use the hot dense propagators for quarks and gluons in 2×2 matrix in TFD[9]. Among them the hot propagator of quark has the form

$$i\Delta_{11}(p) = -i\Delta_{22}(p) = p\left(\frac{1}{p^2 - i\epsilon} - 2\pi(\theta(p_0)e^{x_p/2}n_f(x_p) + \theta(-p_0)e^{-x_p/2}n_f(-x_p))\delta(p^2)\right)$$

$$i\Delta_{12}(p) = -i\Delta_{21}(p) = -2\pi \not p e^{-\beta\mu}(\theta(p_0)e^{x_p/2}n_f(x_p) + \theta(-p_0)e^{-x_p/2}n_f(-x_p))\delta(p^2)$$
(12)

where

$$n_f(x_p) = \frac{1}{e^{x_p} + 1}, \quad x_p = \beta(p_0 + \mu).$$

And for the gluons

$$\Delta_{11}^{L}(q) = -i\Delta_{22}^{L}(q) = \frac{1}{q^{2} - m_{0}^{2} - i\epsilon} - 2\pi i\delta(q^{2} - m^{2})n_{B}(q) = \Delta_{0}^{L} + \Delta_{\beta}^{L},$$

$$\Delta_{L}^{12}(q) = 2\pi i\delta(q^{2} - m_{0}^{2})n_{B}(q)e^{-\beta|q_{0}|/2},$$

$$\Delta_{11}^{T}(q) = Re\frac{1}{(q_{0} - i\nu_{T})^{2} - q^{2}} - 2\pi iIm\frac{1}{(q_{0} - i\nu_{T})^{2} - q^{2}}n_{B}(q),$$

$$\Delta_{11}^{T}(q_{0} \to 0, q) = \frac{1}{q^{2} - \nu_{T}^{2} - i\epsilon} - 2\pi i\delta(q^{2} - \nu^{2})n_{B}(q),$$

$$\Delta_{T}^{12}(q) = 2Im\Delta_{T}n_{B}(q)e^{-\beta|q_{0}|/2}$$

$$= \frac{1}{i|q_{0}|} \left[\frac{1}{(q_{0} - i\nu_{T})^{2} - Q^{2}} - \frac{1}{(q_{0} + i\nu_{T})^{2} - Q^{2}} \right]n_{B}(q)e^{-\beta|q_{0}|/2},$$
(13)

where n_B is the Bose distribution function and for soft mementum q

$$n_B(q) = \frac{1}{e^{\beta|q_0|} - 1} \sim \frac{T}{|q_0|}, \quad n_B(p+q) \sim n_B(p).$$

It is known that one can get the imginary part of the retard Green function of the quark self-energy from the imaginary part of (1-2) type Green function, which is very convenient to calculate in TFD[10]

$$Im\bar{\Sigma} = \frac{e^{\beta\mu/2}}{\sin 2\phi_{p+\mu}} Im\Sigma_{12},\tag{14}$$

where

$$\sin \phi_{p+\mu} = \frac{\theta(p_0)e^{-x_p/4} + \theta(-p_0)e^{x_p/4}}{\sqrt{e^{x_p/2} + e^{-x_p/2}}},$$

$$\cos \phi_{p+\mu} = \frac{\theta(p_0)e^{x_p/4} + \theta(-p_0)e^{-x_p/4}}{\sqrt{e^{x_p/2} + e^{-x_p/2}}}.$$
(15)

Then one can obtain

$$ImTr(p\Sigma) = 4g^{2}C_{f}T \int \frac{d^{D-1}q}{(2\pi)^{2}}|p|^{2}\delta((p+q)^{2})(\frac{1}{q^{2}+\nu^{2}} - \frac{1}{q^{2}+m^{2}} - (1-\xi)\frac{\cos^{2}\theta}{q^{2}}).$$
(16)

Substituting eq(16),into eq(2), and assuming the transfer momentum q is soft: $0 < q \sim gT < T, q/P \sim g$ we obtain

$$\begin{split} \Gamma_{trsp,q} &= \frac{g^2 C_f T}{4\pi P^2} \int dq \int_{-1}^1 dz q^3 (1-z^2) \delta(z+\frac{q}{2P}) (\frac{1}{q^2+\nu^2} - \frac{1}{q^2+m^2} - (1-\xi) \frac{z^2}{q^2}) \\ &= \frac{g^2 C_f T}{4\pi P^2} \int dq q^2 (1-O(\frac{q^2}{4P^2})) (\frac{q^2}{q^2+\nu^2} - \frac{q^2}{q^2+m^2} - (1-\xi)O(\frac{q^2}{4P^2})) \end{split}$$

which shows that the gauge dependent part is suppressed by the square of the coupling constant g^2 by evaluating the integration over q in $0 < q \sim gT < T$, we obtain:

$$\Gamma_{trsp,q} = \frac{g^2 C_f T}{8\pi P^2} \left(m^2 \ln \frac{T^2 + m^2}{m^2} + \frac{\nu^2}{2} \ln \frac{\nu^2}{T^2 + \nu^2} \right). \tag{17}$$

The transport interaction rate of gluon can be obtained in a similar way from the gluon self-energy, and it was found that

$$\Gamma_{trsp,g} = \frac{N}{C_f} \Gamma_{trsp,q}.$$
(18)

One can evaluate the quark and gluon energy density in QGP via the vaccum graphs in hot QCD both at finite temperature and chemical potential:[1]

$$\varepsilon_g = 16 \times \frac{\pi^2}{30} T^4 \left(1 - \frac{15\alpha_s}{4\pi} \right)$$

$$\varepsilon_q = 6N_f \left(\frac{7\pi^2}{120} T^4 \left(1 - \frac{50\alpha_s}{21\pi} \right) + \frac{1}{4} \mu^2 T^2 + \frac{\mu^4}{8\pi^2} \left(1 - \frac{2\alpha_s}{2\pi} \right) \right). \tag{19}$$

By making use of eqs(1),(2),(19), and assuming $p \simeq 3T$, $\nu_T \sim N\alpha_s T[8]$ we can get the shear viscosity coefficient of quarks for two flavors and gluons respectively

$$\eta_q = \frac{\frac{27}{5\pi} \left(\frac{7\pi^2}{120} T^3 \left(1 - \frac{50\alpha_s}{21\pi}\right) + \frac{1}{4}\mu^2 T + \frac{\mu^4}{8\pi^2 T} \left(1 - \frac{2\alpha_s}{2\pi}\right)\right)}{\alpha_s^2 \left(4/3 + \frac{1}{\pi^2} \frac{\mu^2}{T^2}\right) \left(-\ln \alpha_s + \ln\left(\frac{1}{4\pi(4/3 + \frac{1}{2}\frac{\mu^2}{T^2})} + \alpha_s\right) + A(\nu)\right)}.$$
 (20)

$$\eta_g = \frac{\frac{16}{5\pi} (\frac{\pi^2}{30}) T^3 (1 - \frac{15\alpha_s}{4\pi})}{\alpha_s^2 (4/3 + \frac{1}{\pi^2} \frac{\mu^2}{T^2}) (-\ln \alpha_s + \ln(\frac{1}{4\pi (4/3 + \frac{1}{\pi^2} \frac{\mu^2}{T^2})} + \alpha_s) + A(\nu))}.$$
 (21)

$$A(\nu) = \frac{\nu^2}{m^2} \ln \frac{\nu^2}{\nu^2 + T^2} \sim \frac{N_c^2 \alpha_s}{4\pi (4/3 + \frac{1}{-2} \frac{\mu^2}{T^2})} \ln(\alpha_s^2 \frac{N_c^2}{1 + N_c^2 \alpha_s^2}).$$
(22)

In order to compare with previous calculations, one may come back to vanishing quark chemical potential case and not take the gluon damping rate into account, namely substituting $A(\nu) = 0$ in eqs(20)-(22), then one obtains the shear viscosity coefficient of QGP with two quark flavors at vanishing quark chemical potential without including the finite width effect:

$$\eta = \frac{T^3}{\alpha_s^2} \left[\frac{0.25(1 - \frac{50\alpha_s}{21\pi})}{\ln(\frac{0.6 + \alpha_s}{\alpha_s})} + \frac{0.73(1 - \frac{15\alpha_s}{4\pi})}{\ln(\frac{0.6 + \alpha_s}{\alpha_s})} \right],\tag{23}$$

which agrees with the previous result in ref.3 beyond the leading logarithm approximation in the weak coupling limit except a factor 2 due to the definition. At leading order and leading logarithm approximation, one can cast eq(23) into

$$\eta = 0.98 \frac{T^3}{\alpha_s^2 \ln 1/\alpha_s}.$$
 (24)

The coefficient c=0.98 is remarkably close to the one found by Thoma c=1.02 [3] and the one found by Baym et al.[2], the reason of the difference is we used $< p_q > \sim < p_g > \sim 3T$ other than $< p_q > \sim 3.2T$, $< p_g > \sim 2.7T$.

3 Numerical analysis and discussion

Before our numerical analysis, we consider the running behavior of the coupling constant g. In principle the running coupleing constant is governed by the renormalarization equations of QCD at finite temperature and chemical potential, which is still under investigation. Hereby we only use the following result [12]:

$$\alpha(T,\mu) = \frac{12\pi}{(33 - 2n_f) \ln \frac{0.8\mu^2 + 15.622T^2}{\Lambda_s^2}},$$
(25)

where is the QCD papameter, and we choose $\Lambda_s = 0.1 GeV$ as usual. And n_f is the number of flavor, we will only consider two flavors.

Substituting the running coupling constant eq(25) into egs(20)-(22), we obtain the experessions of the shear viscosity coefficients as functions of temperature and chemical potential. So we can plot the curves of the quark and gluon viscosity coefficients against temperature in Fig.2(a) and Fig. 3(a) for different quark chemical potentials $\mu = 0, 0.2, 0.4 GeV$ with and without including the gluon damping effect in QGP respectively. From Fig.2(a) one can find the quark chemical potential effect may enhance the quark viscosity coefficient tremendously because the increase of quark energy density in QGP, while the chemical potential effect on the gluon viscosity is almost negligible. From Fig. 3(a) we find that the three curves of gluon viscosity coefficient against T at different chemical potential almost meet together both with and without taking into acount the gluon finite width. On the

other hand the gluon damping effect causes large enhancements to the shear viscosities both for quark and gluon. The reason is that the damping effect has decreased their transport interaction rates, and hence increase their mean free paths. This qualitatively agrees with the analyses in ref.4 for the nuclear matter.

Fig.2(b) and Fig.3(b) show the temperature dependence of the scaled viscosity coefficients η/T^3 for different quark chemical potentials $\mu=0,0.2,0.4 GeV$ with and without including the gluon damping effect . Our result agrees with the Kubo formula result in ref.2 $\eta/T^3 \geq 2.6/\alpha_s$ at vanish baryon density, but our result is much bigger than the lattice estimate near the critical temperature in ref.2 . Fig.2(b) and Fig.3(b) showes at vanish chemical potential the curves of scaled viscoisity coefficients are no longer flat lines because of the running coupling constant. On the other hand, the tendencies are quite different between the scaled viscoisity of quark and gluon. The reason is the quark chemical potential plays different roles in them. Neverthless, the finite width still cause considerable enhancement to both the scaled viscosity coefficients

Now we study how the shear viscosity coefficients vary with the coupling constant. We plot the curves of the scaled viscosity coefficients η/T^3 against the coupling constant at a fixed temperature T=300MeV and different quark chemical potentials $\mu=0,0.2,0.4GeV$ with and without including the gluon damping effect in Fig.2(c) and Fig.3(c). The curves are almost above the Navier-Stockes Regime and in agreement with Thoma's result. Also the tendencies are quite different between the scaled viscosity of quark and gluon via the coupling constant because of quark chemical potential plays different roles in them. However , the finite width still cause considerable enhancement to both the scaled viscosity coefficients. One interesting thing

is that, although our calculations are valid for weak coupling limit g < 1, Fig.2(c) and Fig.3(c) show that the results can be extrapolated to higher coupling constant at fixed temperatur T = 300 MeV, as predicted in ref.3 at least for quantities of energetic particles with E >> T.

4 Summary and Conclusions

We have examined the quark and gluon shear viscosity behaviors by real time QCD both at finite temperature and baryon density in the quark gluon plasma in which both Debye screening and damping or finite width are regarded as important underlying features. Also the running feature of the coupling constant is accounted for. We have seen that both the quark and gluon shear viscosity coefficients are increased substantially, due to the effects of the finite width of transverse gluons. Meanwhile all the scaled shear viscosity coefficients are increased in comparison with the previors results, in which the finite widtheffect was not accounted for.

We have also examined the quark chemical potential effects to the shear viscosity coefficients in a straight forward way. It also enhances the shear viscosity coefficients of QGP consiberably, but the enhancements are smaller than that caused by the finite width effect. On the other hand, we have seen the tendencies of the quark viscosity coefficients, especially the scaled ones, differ quite substantially from that of the gluon. This is because the baryon density plays different roles in quark and gluon shear viscosity coefficients.

We note that If we remove the quark chemical potential and finite width the results will be in good agreement with previous calculations [2,3,13].

We conclude that both the gluon damping rate and quark chemical potential effects have a considerable influence on the dissipative processes of QGP. This dissipation cannot be neglected in hydrodynamic descriptions of the expansion phase of QGP in ultrarelativistic heavy ion collisions.

Acknowledgments

This work is supported partly by the National Natural Science Funds of China. Hou Defu wants to thank the Deutsche Forschungsgemeinschaft (DFG) for supports. The authors are indebted to Peter Henning and Ulrich Heinz for valuble discussion and comments, and which to thank Liu Lianshou for his help.

Reference

- [1] Müller, in NATO ASI Series B, Physics Vol.303(Plenum Press, NewYork,
 London,1992); U.Heinz, K.Kajantie and T.Toimela, Annals of Phys. 176,218(1987);
 J.-P. Blaizot, Nucl. Phys. A566, (1994)333c.
- [2] A.Hosoya and K.K. Kajantie, Nucl.Phys.B250,666(1985); P. Danielewicz and M.Gyulassy, Phys.Rev.D31,53(1985);
 G.Baym, H. Monien, C.J.Pethick and D.G.Ravenha, Phys.Rev.Lett.64, 1867(1990).
- [3] M.H.Thoma, Phys.Rev.**D49**(1994)451; M.H.Thoma, Phys.Lett**B**(1991)144.
- [4] P.A.Henning, Nucl. Phys. **A567**,844(1994).
- [5] H. Vija and M.H.Thoma Phys.Lett**B342**,212(1995).
- [6] N.P.Landsman, and Ch.G.Van Weert, Phys.Rep. 145,141(1987).
- [7] P.Henning Phys.Rep.253,235 (1995); Hou Defu, Li Jiarong, Z.Phys.C71,503(1996)
 Hou Defu, S. Ochs, Li Jiarong, Phys. Rev.D54,(1996)(in press)
- [8] R.D.Pisarski, Phys.Rev.Lett. 63,1129(1989); E.Braaten, R.D.Pisarski, Phys. Rev.D42, 2156(1990), Phys.Rev.Lett., 64,1338(1990).
- [9] R.Kobes, Phys. Rev. **D42**,562 (1990); Phys. Rev. **D43**,1269(1991).
- [10] Y.Fujimoto, M. Morikawa and M. Sasaki, Phys. Rev. D33,590(1986).
- [11] Y. Fujimoto and Hou Defu, Phys. Lett. **B335**, (1994)87.
- [12] C.P.Singh B.K.Patra, and Saeed Uddin, Phys.Rev. $\mathbf{D49},4023(1994)$.
- $[{\bf 13}\]$ P.Rehberg, S.P. Klevansky and J.Hüfner, Nucl. Phys.A608 ,356(1996).

Figure captions

- Fig.1 The resummed one-loop quark self-energy graph
- Fig.2(a) The quark viscosity coefficient as a function of the temperture for $\mu=0,0.2,0.4$ (bottom to top) without (thin solid lines in lower part) and with (thick solid lines in upper part)including the gluon damping effect .
- **Fig.2(b)** The scaled quark viscosity coefficient η/T^3 as a function of the temperture for $\mu=0,0.2,0.4$ (bottom to top) without (thin solid lines in lower part) and with (thick solid lines in upper part)including the gluon damping effect .
- **Fig.2(c)** The scaled quark viscosity coefficient η/T^3 as a function of coupling constant α at fixed temperature T=300MeV for $\mu=0,0.2,0.4$ (bottom to top) without (thin solid lines in lower part) and with (thick solid lines in upper part)including the gluon damping effect .
- Fig.3(a) The gluon viscosity coefficient as a function of the temperture for $\mu=0,0.2,0.4$ (meet together) without (thin solid lines in lower part) and with (thick solid lines in upper part)including the gluon damping effect .
- Fig.3(b) The scaled gluon viscosity coefficient η/T^3 as a function of the temperture for $\mu=0,0.2,0.4$ (bottom to top) without (thin solid lines in lower part) and with (thick solid lines in upper part)including the gluon damping effect .
- Fig.3(c) The scaled gluon viscosity coefficient η/T^3 as a function of coupling constant α at fixed temperature T=300MeV for $\mu=0,0.2,0.4$

(bottom to top) without (thin solid lines in lower part) and with (thick solid lines in upper part)including the gluon damping effect .

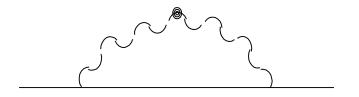


Fig. 1

Fig. 2 Fig. 3

